Modeling the bacterial self-organization in a circular container along the contact line as detected by bioluminescence imaging

Romas Baronas[a], **Remigijus Šimkus**[b]

[a]Faculty of Mathematics and Informatics, Vilnius University
Naugarduko str. 24, LT-03225 Vilnius, Lithuania
romas.baronas@mif.vu.lt

[b]Vilnius University Institute of Biochemistry
Mokslininkų str. 12, LT-08662 Vilnius, Lithuania
remigijus.simkus@bchi.vu.lt

Received: 24 February 2011 / **Revised:** 2 June 2011 / **Published online:** 19 September 2011

Abstract. This paper presents a one-dimensional-in-space mathematical model of a bacterial self-organization in a circular container along the contact line as detected by quasi-one-dimensional bioluminescence imaging. The pattern formation in a luminous *Escherichia coli* colony was modeled by the nonlinear reaction-diffusion-chemotaxis equations in which the reaction term for the cells is a logistic (autocatalytic) growth function. By varying the input parameters the output results were analyzed with a special emphasis on the influence of the model parameters on the pattern formation. The numerical simulation at transition conditions was carried out using the finite difference technique. The mathematical model and the numerical solution were validated by experimental data.

Keywords: reaction-diffusion, chemotaxis, pattern formation, mathematical modeling, whole-cell biosensor.

1 Introduction

The survival of many microscopic as well as large organisms often depends on their ability to move within an environment by responding to internal and external signals. Microorganisms respond to different chemicals found in their environment by migrating either toward or away from them. The directed movement of microorganisms in response to chemical gradients is called chemotaxis [1]. Chemotaxis plays crucial role in a wide range of biological phenomena. Within the embryo, chemotaxis affects avian gastrulation and patterning of the nervous system. The same mechanisms are utilized during cancer growth, allowing tumour cells to invade into healthy tissue or drive new blood vessel growth (angiogenesis) [2]. Although chemotaxis has been observed in many bacterial species, *Escherichia coli* is one of the mostly studied examples. *E. coli* respond to the chemical stimulus by alternating the rotational direction of their flagella [1].

Bacterial species including *E. coli* have been observed to form various patterns under different environmental conditions [3–5]. Populations of bacteria are capable of self-organization into states exhibiting strong inhomogeneities in density [6, 7].

Starting from the fifties various mathematical models have been successfully used as important tools to study the mechanisms of chemotaxis [8]. The patterns of bacterial chemotaxis have been studied theoretically on the basis of Patlak–Keller–Segel model [9–11]. A comprehensive review on the mathematical modeling of chemotaxis has been presented by Hillen and Painter [12].

Recently, the spatiotemporal patterns in the fluid cultures of *E. coli* have been observed by employing lux-gene engineered cells and a bioluminescence imaging technique [13, 14]. However, the actual mechanisms governing the formation of bioluminescence patterns remained unclear with respect to the investigations into bacterial self-organization and transport. Over the last decade, lux-gene engineered bacteria have been successfully used to develop whole cell-based biosensors [15].

In this paper, we investigate the bacterial self-organization in a small circular container along the contact line as detected by quasi-one-dimensional bioluminescence imaging. The aim of the current study was to develop a mathematical model describing patterns of bioluminescence in the fluid cultures of *E. coli*. Assuming that the luminescence in experiments is proportional to the cell density, the pattern formation in a luminous *E. coli* colony was modeled by the nonlinear reaction-diffusion-chemotaxis equations in which the reaction term for the cells is a logistic (autocatalytic) growth function. Due to the accumulation of luminous cells near the contact line, the essentially three-dimensional processes were mathematically described in one-dimensional domain (quasi-one dimensional ring). By varying the input parameters the output results were analyzed with a special emphasis on the influence of the model parameters on the pattern formation. The numerical simulation at transition conditions was carried out using the finite difference technique [16]. The mathematical model and the numerical solution were validated by experimental data.

2 Mathematical modeling

A representative class of mathematical models based on advection-reaction-diffusion equations has been developed for modeling of pattern formation in bacterial colonies [3,4,17–24]. The system of coupled partial differential equations introduced by Keller and Segel remains among the most widely used [9, 10, 12].

2.1 Governing equations

According to the Keller and Segel approach, translating the main biological processes into a mathematical model leads to a system of two conservation equations [9, 10, 20],

$$\begin{aligned} \frac{\partial n}{\partial t} &= \nabla \left(D_n \nabla n - h(n,c) n \nabla c \right) + f(n,c), \\ \frac{\partial c}{\partial t} &= \nabla \left(D_c \nabla c \right) + g_p(n,c) n - g_d(n,c) c, \quad \mathrm{x} \in \Omega \subset \mathbb{R}^n, \ \ t > 0, \end{aligned} \tag{1}$$

where x and t stand for space and time, $n(\mathrm{x}, t)$ is the cell density, $c(\mathrm{x}, t)$ is the chemoattractant concentration, D_n and D_c are the diffusion coefficients usually assumed to be constant, $f(n, c)$ stands for cell growth and death, $h(n, c)$ is the chemotactic sensitivity, g_p and g_d describe the production and degradation of the chemoattractant [9]. Instantiating f, g_p, g_d and h with concrete expressions leads to particular models for chemotaxis [12,25].

The function $h(n, c)$ controls the chemotactic response of the cells to the chemoattractant. The form of $h(n, c)$ ultimately depends on the sensitivity of cells at different concentrations of the attractant [26]. In the simplest form, the sensitivity of cells to attractant is assumed to be independent of the chemoattractant concentration, i.e. $h(n, c)$ is constant, $h(n, c) = k_1$. Since the bacterial current flow declines at low chemical concentrations and saturates at high concentrations, Lapidus and Schiller derived the following expression of the chemotactic sensitivity for *E. coli*: $h(n, c) = k_1/(k_2 + c)^2$, where k_1 and k_2 are constants [17, 20, 27].

The cell growth is usually assumed to be logistic, i.e. $f(n, c) = k_3 n(1 - n/n_0)$, where k_3 is the growth rate of the cell population, and n_0 is the cell density under steady-state conditions. k_3 and n_0 are usually constant [3].

A number of chemoattractant production functions have been used in chemotactic models [12]. Usually, a saturating function of the cell density is used indicating that, as the cell density increases, the chemoattractant production decreases. The Michaelis–Menten function is widely used to express the production rate, $g_p(n, c) = k_4/(k_5 + n)$ [9, 18, 26]. Tyson et al. [20] introduced a n^2 dependence for sufficiently rapid increase in production of attractant when modeling *E. coli* pattern formation, $g_p(n, c) = k_4 n/(k_5 + n^2)$. The degradation or consumption of the chemoattractant is typically linear, $g_d(n, c) = k_6$, where k_6 is a constant. Values of k_4, k_5 and k_6 are not exactly known [20].

When modeling the bacterial self-organization in a circular container along the contact line [13, 14], the mathematical model can be defined on a one dimensional space - the circumference of the vessel. Inserting the concrete expressions of f, g_p, g_d and h to system (1) leads to the governing equations of the cell kinetics model with nonlinear signal kinetics and signal dependent sensitivity,

$$\begin{aligned} \frac{\partial n}{\partial t} &= D_n \Delta n - \nabla \left(\frac{k_1 n}{(k_2 + c)^2} \nabla c \right) + k_3 n \left(1 - \frac{n}{n_0} \right), \\ \frac{\partial c}{\partial t} &= D_c \Delta c + \frac{k_4 n^p}{k_5 + n^p} - k_6 c, \quad x \in (0, l), \;\; t > 0, \end{aligned} \tag{2}$$

where Δ is the Laplace operator formulated in the one-dimensional Cartesian coordinate system, p stands for the production dependence order of attractant, p equals 1 or 2, and l is the length of the contact line, i.e. the circumference of the vessel (a circle). Assuming R as the vessel radius, $l = 2\pi R$, $x \in (0, 2\pi R)$.

2.2 Initial and boundary conditions

We assume a possibly non-uniform initial distribution of cells as well as of the chemoattractant,

$$n(x, 0) = n_{0x}(x), \quad c(x, 0) = c_{0x}(x), \quad x \in [0, l], \tag{3}$$

where $n_{0x}(x)$ and $c_{0x}(x)$ stand for the initial ($t = 0$) cell density and the chemoattractant concentration, respectively.

For the bacterial simulation on a continuous circle of the length l of the circumference, we apply the following boundary conditions ($t > 0$):

$$n(0,t) = n(l,t), \quad c(0,t) = c(l,t), \quad \frac{\partial n}{\partial x}\Big|_{x=0} = \frac{\partial n}{\partial x}\Big|_{x=l}, \quad \frac{\partial c}{\partial x}\Big|_{x=0} = \frac{\partial c}{\partial x}\Big|_{x=l}. \quad (4)$$

2.3 Dimensionless model

In order to define the main governing parameters of the mathematical model (2)–(4) [5, 12, 26], a dimensionless mathematical model has been derived by setting

$$\begin{gathered} u = \frac{n}{n_0}, \quad v = \frac{k_5 k_6 c}{k_4 n_0^p}, \quad t^* = \frac{k_6 t}{\gamma}, \quad x^* = \sqrt{\frac{k_6}{D_c \gamma}}x, \quad D = \frac{D_n}{D_c}, \\ \chi = \frac{k_1 k_4 n_0^p}{k_2^2 k_5 k_6 D_c} = \frac{k_1 \alpha}{k_2 D_c}, \quad r = \frac{k_3}{k_6}, \quad \alpha = \frac{k_4 n_0^p}{k_2 k_5 k_6} = \frac{k_4 \beta}{k_2 k_6}, \quad \beta = \frac{n_0^p}{k_5}. \end{gathered} \quad (5)$$

Dropping the asterisks for algebraic simplicity, the dimensionless governing equations then become

$$\begin{aligned} \frac{\partial u}{\partial t} &= D\frac{\partial^2 u}{\partial x^2} - \frac{\partial}{\partial x}\left(\frac{\chi u}{(1+\alpha v)^2}\frac{\partial v}{\partial x}\right) + \gamma r u(1-u), \\ \frac{\partial v}{\partial t} &= \frac{\partial^2 v}{\partial x^2} + \gamma\left(\frac{u^p}{1+\beta u^p} - v\right), \quad x \in (0,1), \ \ t > 0, \end{aligned} \quad (6)$$

where u is the dimensionless cell density, v is the dimensionless chemoattractant concentration, α stands for the signal-dependent (receptor) sensitivity, β stands for saturating of the signal production, and γ stands for the spatial and temporal scale.

For the dimensionless simulation the initial conditions were

$$u(x,0) = 1 + \varepsilon(x), \quad v(x,0) = 0, \quad x \in [0,1], \quad (7)$$

where $\varepsilon(x)$ is a 20% random uniform spatial perturbation.

The boundary conditions (4) transform to the following dimensionless equations ($t > 0$):

$$u(0,t) = u(1,t), \quad v(0,t) = v(1,t), \quad \frac{\partial u}{\partial x}\Big|_{x=0} = \frac{\partial u}{\partial x}\Big|_{x=1}, \quad \frac{\partial v}{\partial x}\Big|_{x=0} = \frac{\partial v}{\partial x}\Big|_{x=1}. \quad (8)$$

The dimensionless model (6)–(8) involves six parameters (D, χ, r, α, β and γ) while the corresponding dimensional model (2)–(4) contains even ten (D_n, D_c, $k_1, k_2, \ldots, k_6$, n_0 and l) parameters.

According to the classification of chemotaxis models [12] the dimensionless model of the pattern formation is a combination of the signal-dependent sensitivity (M2a), the saturating signal production (M6) and the cell kinetics (M8) models.

3 Numerical simulation

The mathematical model (2)–(4), as well as the corresponding dimensionless model (6)–(8), of the bacterial self-organization has been defined as an initial boundary value problem based on a system of nonlinear partial differential equations. There exist theoretical methods which may yield helpful analytical results into the behavior of the system, e.g., linearization, stationary solutions, homogeneous solutions, stability analysis [5,11,28,29]. However, in the general case, because of the nonlinearity of the problem, no analytical solutions could be derived [5, 11, 28, 29]. Hence the numerical simulation of the bacterial self-organization was used.

The simulations were carried out using the finite difference technique [16]. To find a numerical solution of the problem we introduced a uniform discrete grid with 250 points and the dimensionless step size 0.004 in the space direction, $250 \times 0.004 = 1$. A constant dimensionless step size 10^{-6} was also used in the time direction. An explicit finite difference scheme has been built as a result of the difference approximation [16,30]. The digital simulator has been programmed by the authors in JAVA language [31].

Assuming that the luminescence in experiments is proportional to the cell density, the mathematical model and the corresponding numerical model were validated by computational simulation of bioluminescence patterns observed in small circular containers made of glass [14]. Fig. 1 shows typical top view bioluminescence images of bacterial cultures illustrating an accumulation of luminous bacteria near the contact line. In general, the dynamic processes in unstirred cultures are rather complicated and need to be modeled in three dimensional space [13, 14, 32, 33]. Nevertheless, the accumulation of luminous cells near the contact line implies that the essentially three-dimensional processes may be approximated in one dimension (quasi-one dimensional rings in Fig. 1). The typical space-time plot of quasi-one-dimensional bioluminescence intensity is shown in Fig. 2.

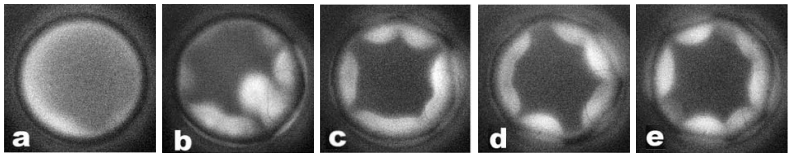

Fig. 1. Top view bioluminescence images of the bacterial cultures in the cylindrical vessel at different time moments: 5 (a), 20 (b), 40 (c), 60 (d) and 90 (e) min [14].

The patterns of bioluminescence observed during the long run experiments can be characterized by the formation of meandering traveling waves and relative stability of the corresponding wave number (number of waves along the contact line). The characteristic wave speed of the bioluminescent waves is $\sim 7\mu\mathrm{m/s}$. Qualitatively, the observed space-time plot exhibits the so-called merging and emerging dynamics in chemotaxis [12].

By varying the model parameters the output results were analyzed with a special emphasis on simulating a spatiotemporal pattern similar to the experimentally obtained pattern shown in Fig. 2. Fig. 3 shows the results of the informal pattern fitting.

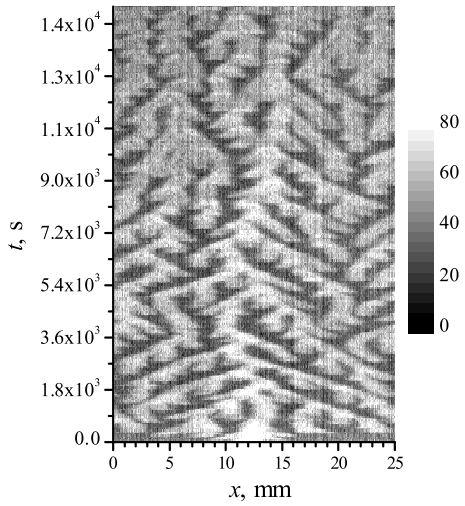

Fig. 2. Space-time plot of bioluminescence measured in a circular container along the contact.

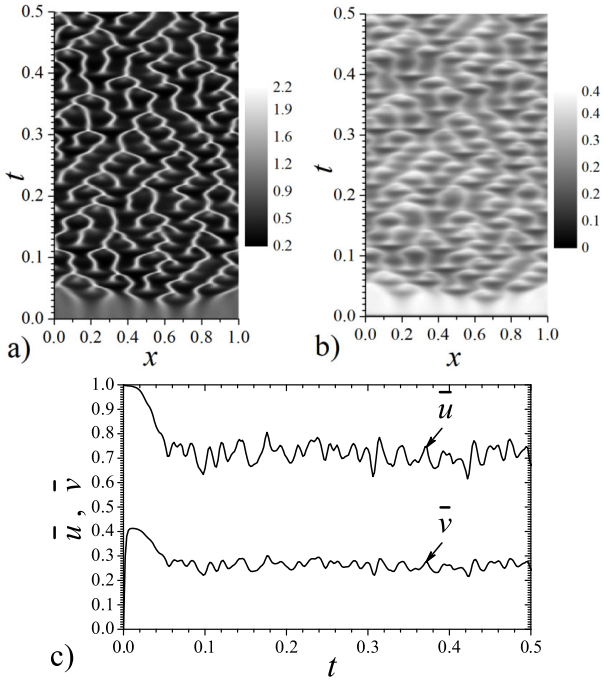

Fig. 3. Simulated space-time plot of the dimensionless cell density u (a), the chemoattractant concentration v (b) and the corresponding values $\bar{u}$ and $\bar{v}$ averaged on circumference of the vessel (c) at values defined in (10).

Fig. 3 presents numerically simulated space-time plots of the dimensionless cell density u (a), the chemoattractant concentration v (b). The dynamics of the corresponding values of $\bar{u}$ and $\bar{v}$ averaged on circumference of the vessel are depicted in Fig. 3(c),

$$\bar{u}(t) = \int_0^1 u(x,t)dx, \quad \bar{v}(t) = \int_0^1 v(x,t)dx\,. \tag{9}$$

The dynamics of the bacterial population was simulated at the following values of the model parameters:

$$D = 0.1, \quad \chi = 9.2, \quad r = 1, \quad \alpha = 0.7, \quad \beta = 1.4, \quad \gamma = 625, \quad p = 2\,. \tag{10}$$

Values (10) of the model parameters were determined experimentally by changing input parameters and aiming to achieve a meandering wave pattern comparable to the one shown in Fig. 2. Taking into account the transformation (5) of the variables, we can determine values of the dimensional parameters. Having the value of k_6 we could have a direct relation between the dimensional time and the dimensionless time. Unfortunately, no precise value of k_6 is known [5, 25]. Assuming the duration (250 min $=$ 15000 s) of a physical experiment correlates with the dimensionless duration (0.5), we obtain $k_6 = 0.5 \times 625/15000 = 0.02\ \mathrm{s}^{-1}$. Having this estimation and the relation between the dimensional ($l = 25$ mm) and the dimensionless (1) length, we found the diffusion coefficients, $D_c = k_6 l^2/\gamma = 0.02 \times 2.5^2/625 = 2 \times 10^{-4}\mathrm{cm}^2/\mathrm{s}$, $D_n = 0.1 D_c = 2 \times 10^{-5}\mathrm{cm}^2/\mathrm{s}$. This value of the diffusion coefficient D_n for *E. coli* cells in a liquid medium is notably greater than that ($2-4\times10^{-6}\mathrm{cm}^2/\mathrm{s}$) determined by Berg and Turner [34]. However, it fits perfectly with the estimate ($2.2 \pm 0.15 \times 10^{-5}\mathrm{cm}^2/\mathrm{s}$) obtained by Perry [21]. According to Lin et al. [35], the diffusion coefficient of *E. coli* can be even several times greater. So, values (10) seems to be admissible for the simulation of the pattern formation in an *E. coli* colony. A more detailed interpretation of the parameters of the model will be given in the biological-biochemical literature (Simkus and Baronas, in preparation).

Due to a relatively great number of model parameters, there is no guarantee that the values (10) lead to the best agreement of simulation results with the pattern shown in Fig. 2. In multiple simulation runs, very similar patterns were achieved at different values of the parameters. The linearization and the stability analysis of homogenous solutions of the chemotaxis-diffusion equations (Keller–Segel model) showed similar effects [11, 28, 29]. Often, an increase in one parameter can be compensated by decreasing or increasing another one. Because of this, it is very important to investigate the dependence of the pattern formation on the model parameters.

4 Results and discussion

By varying the input parameters the output results were analyzed with a special emphasis on the influence of the model parameters on the spatiotemporal pattern formation in the luminous *E. coli* colony.

4.1 The significance of the signal-dependent sensitivity

The chemotactic response to chemical gradients is mediated through the external detection of a signal and its subsequent transduction to internal pathways [5]. A common feature of many chemotaxis models is to build some of this complexity into the equations through a signal-dependent chemotactic sensitivity function [12]. One of the most commonly utilized form is the "receptor" form, where the dimensionless chemotactic sensitivity is expressed by $\chi/(1+\alpha v)^2$. According to this approach, at high concentrations of v, the receptors may become fully occupied and the cell is unable to further resolve a gradient [12, 36]. Nevertheless, many authors use the constant chemotactic sensitivity, i.e. $\alpha = 0$ [12, 18, 26].

In order to investigate the dependence of the signal-dependent sensitivity on the pattern formation, the space-time plots were simulated at the different values α adjusting other parameters (mainly, χ) so that to hold the pattern shown in Fig. 3(a). The simulated patterns are depicted in Fig. 4.

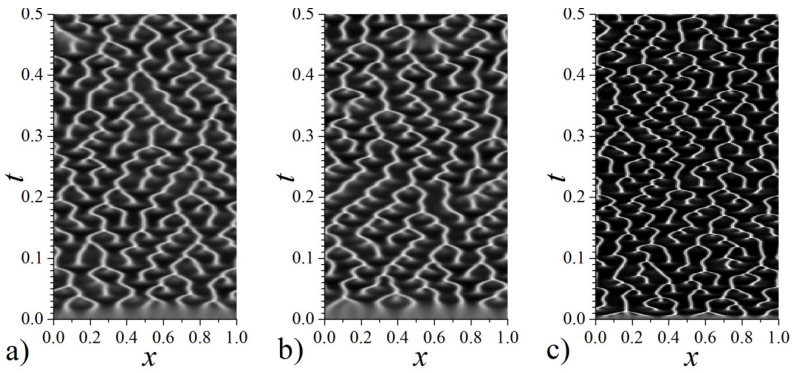

Fig. 4. Space-time plots of the dimensionless cell density u simulated at different values of α and χ: $\alpha = 0$, $\chi = 6.2$ (a); $\alpha = 0.35$, $\chi = 7.7$ (b); $\alpha = 0$, $\chi = 9.2$ (c). Values of other parameters are as defined in (10).

Fig. 4 shows how a reduction in value of α can be compensated by decreasing in χ. The complete reduction of α-parameter (α reduces from 0.7 to 0) and the decrease in χ-value from 9.2 to 6.2 led to a change in the pattern from Fig. 3(a) to Fig. 4(a). When comparing the patterns shown in these figures, one can see a noticeable difference only in the initial stage of the pattern formation (up to $t \approx 0.04$). Thus, a constant function of the chemotactic response ($h(n,c)$ in (2)) can be applied in modeling of the pattern formation in a population along the contact line in a circular container.

The linear dependence of signal-dependent sensitivity on the pattern formation can be also noticed when comparing the space-time plot simulated at intermediate values of α and χ ($\alpha = 0.35$, $\chi = 7.7$, Fig. 4(b)) with the corresponding plots simulated at the marginal values of these parameters, $(\alpha, \chi = (0.7, 9.2)$ (Fig. 3(a)) and $(\alpha, \chi) = (0, 6.2)$ (Fig. 4(a)). All these three patterns look similar.

Fig. 4(c) shows that, in general, the reduction of α noticeably effects the pattern

formation if it is not compensated by decreasing in χ. Nevertheless, the properly choosing of χ-value allows to use the zero value of α (Figs. 3(a) and 4(a)).

4.2 The effect of the attractant production rate

As pointed out in Section 2, a number of chemoattractant production functions have been used in chemotactic models [12, 18, 20]. Usually, it is assumed that the production saturates with increasing cell density. The order n^2 ($p = 2$) as well as n ($p = 1$) dependences for the increase in the attractant production have been widely used [27].

In order to investigate the dependence of the attractant production rate on the pattern formation, the space-time plots were additionally simulated at $p = 1$ and different values of β. The simulated patterns are depicted in Fig. 5.

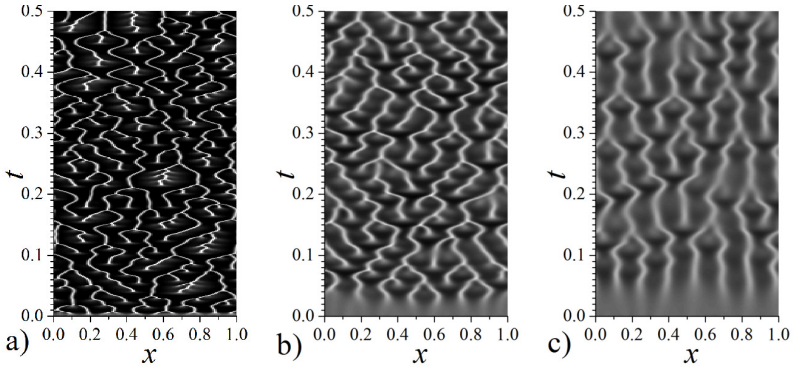

Fig. 5. Space-time plots of the dimensionless cell density u simulated at $p = 1$ and three values of β: 0.3 (a), 0.73 (b), 0.8 (c). Values of other parameters are the same as in Fig. 4(a).

One can see that pattern simulated at $p = 1$ and $\beta = 0.73$ (Fig. 5(b)) is similar to that simulated at $p = 2$ and $\beta = 1.4$ (Fig. 4(b)) keeping other parameters the same. Changing the n^2-order dependence to the n-order dependence for the increase in the attractant production leads to decreasing β-value from 1.4 to 0.73. Fig. 5 shows that the model parameter β plays a key role in a pattern formation. Some additional simulations showed that the pattern obtained experimentally (Fig. 3(a)) can not be simulated at $\beta = 0$.

4.3 A minimal model

Accepting $\alpha = 0$ and $p = 1$, the governing equations (6) were assumed to be minimal for modeling the pattern formation along the contact line in a cellular population. Accepting $\alpha = 0$ and $p = 1$ leads to the following governing equations:

$$\begin{aligned} \frac{\partial u}{\partial t} &= D\Delta u - \chi\nabla(u\nabla v) + \gamma r u(1-u), \\ \frac{\partial v}{\partial t} &= \Delta v + \gamma\left(\frac{u}{1+\beta u} - v\right), \quad x \in (0,1), \;\; t > 0. \end{aligned} \tag{11}$$

The governing equations (11) together with the initial (3) and the boundary (4) conditions form a mathematical model suitable for simulating the pattern formation in a colony of luminous *E. coli*. The patterns shown in Fig. 5 were simulated by the minimal model (11), (3) and (4).

According to the classification of chemotaxis models introduced by Hillen and Painter [12], the minimal model of pattern formation (11) combines two models: the nonlinear signal kinetics model M6 and the cell kinetics model M8. This model has been analyzed by Maini and others [5, 18, 26].

Finally, we would like to clarify the concept of "bacterial self-organization" which is frequently used in biophysical but not microbiological literature [6]. It should be noticed, that prolonged accumulation of planktonic *E. coli* at surfaces can further instigate the formation of biofilms [37]. Therefore, it is likely, that the bacterial self-organization and the biofilm formation should be closely related phenomena, which accompany each other. Our numerical simulations show that the processes detectable by bioluminescence imaging in the culture of *E. coli* are rather fast. The diffusion coefficients, which were used in our calculations, are typical for the liquid suspensions of motile bacteria. These results imply that the majority of the luminous cells are mobile and capable of self-organization in a liquid media. The term "bacterial self-organization" seems to be most relevant [6], when describing the behavior of freshly harvested bacteria. On the other hand, the initiation of the biofilm formation under ageing conditions (hours) is also probable [37]. Seemingly, in our experiments, the number of cells which are attached to the surfaces remains significantly lower than that the number of cells in a liquid phase. In this case the biofilm formation may appear as a low background process of the suggested bacterial self-organization.

5 Conclusions

We have shown that Patlak–Keller–Segel models can be used to describe the formation of bioluminescence patterns representing the self-organization of the bacteria. Due to the accumulation of luminous cells near the contact line (Fig. 1), the patterns of the bioluminescence experiments can be qualitatively described by one-dimensional-in-space Keller–Segel model.

The mathematical model (2)–(4) of the bacterial self-organization along the contact line of the circular container as detected by bioluminescence imaging may be successfully used to investigate the pattern formation in a colony of luminous *E. coli*. The corresponding dimensionless mathematical model (6)–(8) can be used as a framework for numerical investigation of the impact of the model parameters on the pattern formation. Very similar patterns can be obtained at different values of the model parameters (Figs. 3(a), 4(a), (b) and 5(b)).

The governing equations of the model (6)–(8) can be restricted to a minimal model (11) in order to obtain satisfactory agreement with experimental patterns.

The more precise and sophisticated two- and three-dimensional computational models implying the formation of structures observed on bioluminescence images are now under development.

Acknowledgements

R. Baronas acknowledge the support of the European Social Fund under Measure VP1-3.1-ŠMM-07-K "Support to Research of Scientists and Other Researchers (Global Grant)", Project "Developing computational techniques, algorithms and tools for efficient simulation and optimization of biosensors of complex geometry", No. VP1-3.1-ŠMM-07-K-01-073/MTDS-110000-583.

References

1. M. Eisenbach, *Chemotaxis*, Imperial College Press, London, 2004.

2. T.C. Williams, *Chemotaxis: Types, Clinical Significance, and Mathematical Models*, Nova Science, New York, 2011.

3. E.O. Budrene, H.C. Berg, Dynamics of formation of symmetrical patterns by chemotactic bacteria, *Nature*, **376**(6535), pp. 49–53, 1995.

4. M.P. Brenner, L.S. Levitov, E.O. Budrene, Physical mechanisms for chemotactic pattern formation by bacteria, *Biophys. J.*, **74**(4), pp. 1677–1693, 1998.

5. J.D. Murray, *Mathematical Biology: II. Spatial Models and Biomedical Applications*, Springer, Berlin, 3rd edition, 2003.

6. E. Ben-Jacob, I. Cohen, H. Levine, Cooperative self-organization of microorganisms, *Adv. Phys.*, **49**(4), pp. 395–554, 2000.

7. S. Sasaki, Y. Mori, M. Ogawa, S. Funatsuka, Spatio-temporal control of bacterial-suspension luminescence using a PDMS cell, *J. Chem. Engineer. Japan*, **43**(11), pp. 960–965, 2010.

8. C.S. Patlak, Random walk with persistence and external bias, *Bull. Math. Biophys.*, **15**(3), pp. 311–338, 1953.

9. E.F. Keller, L.A. Segel, Model for chemotaxis, *J. Theor. Biol.*, **30**(2), pp. 225–234, 1971.

10. D. Horstmann, From 1970 until present: the Keller-Segel model in chemotaxis and its consequences, *I. Jahresberichte DMV*, **105**(3), pp. 103–165, 2003.

11. P. Romanczuk, U. Erdmann, H. Engel, L. Schimansky-Geier, Beyond the Keller-Segel model. Microscopic modeling of bacterial colonies with chemotaxis, *Eur. Phys. J. Special Topics*, **157**(1), pp. 61–77, 2007.

12. T. Hillen, K.J. Painter, A user's guide to PDE models for chemotaxis, *J. Math. Biol.*, **58**(1–2), pp. 183–217, 2009.

13. R. Šimkus, Bioluminescent monitoring of turbulent bioconvection, *Luminescence*, **21**(2), pp. 77–80, 2006.

14. R. Šimkus, V. Kirejev, R. Meškienė, R. Meškys, Torus generated by *Escherichia coli*, *Exp. Fluids*, **46**(2), pp. 365–369, 2009.

15. S. Daunert, G. Barrett, J.S. Feliciano, R.S. Shetty, S. Shrestha, W. Smith-Spencer, Genetically engineered whole-cell sensing systems: coupling biological recognition with reporter genes, *Chem. Rev.*, **100**(7), pp. 2705–2738, 2000.

16. A.A. Samarskii, *The Theory of Difference Schemes*, Marcel Dekker, New York-Basel, 2001.

17. I.R. Lapidus, R. Schiller, Model for the chemotactic response of a bacterial population, *Biophys. J.*, **16**(7), pp. 779–789, 1976.

18. P.K. Maini, M.R. Myerscough, K.H. Winters, J.D. Murray, Bifurcating spatially heterogeneous solutions in a chemotaxis model for biological pattern generation, *Bull. Math. Biol.*, **53**(5), pp. 701–719, 1991.

19. K. Kawasaki, A. Mochizuki, M. Matsushita, T. Umeda, N. Shigesada, Modeling spatio-temporal patterns generaged by *Bacillus subtilis*, *J. Theor. Biol.*, **188**(2), pp. 177–185, 1997.

20. R. Tyson, S.R. Lubkin, J.D. Murray, Model and analysis of chemotactic bacterial patterns in a liquid medium, *J. Math. Biol.*, **38**(4), pp. 359–375, 1999.

21. N. Perry, Experimental validation of a critical domain size in reaction-diffusion systems with *Escherichia coli* populations, *J. R. Soc. Interface*, **2**(4), pp. 379–387, 2005.

22. M.P. Zorzano, D. Hochberg, M.T. Cuevas, J.M. Gomez-Gomez, Reaction-diffusion model for pattern formation in *E. coli* swarming colonies with slime, *Phys. Rev. E*, **71**(3), 31908, 2005.

23. A. Rabner, E. Martinez, R. Pedhazur, T. Elad, S. Belkin, Y. Shacham, Mathematical modeling of a bioluminescent E. coli based biosensor, *Nonlinear Anal. Model. Control*, **14**(4), pp. 505–529, 2009.

24. M.D. Egbert, X.E. Barandiaran, E.A. Di Paolo, A minimal model of metabolism-based chemotaxis, *PLoS Comput. Biol.*, **6**(12), e1001004, 2010.

25. K.J. Painter, T. Hillen, Spatio-temporal chaos in a chemotactic model, *Physica D*, **240**(4–5), pp. 363–375, 2011.

26. M.R. Myerscough, P.K. Maini, K.J. Painter, Pattern formation in a generalized chemotactic model, *Bull. Math. Biol.*, **60**(1), pp. 1–26, 1998.

27. D.E. Woodward, R. Tyson, M.R. Myerscough, J.D. Murray, E.O. Budrene, H.C. Berg, Spatio-temporal patterns generated by *Salmonella typhimurium*, *Biophys. J.*, **68**(5), pp. 2181–2189, 1995.

28. R. Tyson, L.G. Stern, R.J. LeVeque, Fractional step methods applied to a chemotaxis model, *J. Math. Biol.*, **41**(5), pp. 455–475, 2000.

29. F. Schweitzer, L. Schimansky-Geier, Clustering of "active" walkers in a two-component system, *Physica A*, **206**(3–4), pp. 359–379, 1994.

30. R. Baronas, F. Ivanauskas, J. Kulys, *Mathematical Modeling of Biosensors: An Introduction for Chemists and Mathematicians*, Springer, Dordrecht, 2010.

31. J.E. Moreira, S.P. Midkiff, M. Gupta, P.V. Artigas, M. Snir, R.D. Lawrence, Java programming for high-performance numerical computing, *IBM Syst. J.*, **39**(6), pp. 21–56, 2000.

32. N.A. Hill, T.J. Pedley, Bioconvection, *Fluid Dyn. Res.*, **37**(1–2), pp. 1–20, 2005.

33. C.-Y. Hsu, R. Dillon, A 3D motile rod-shaped monotrichous bacterial model, *Bull. Math. Biol.*, **71**(5), pp. 1228–1263, 2009.

34. H.C. Berg, L. Turner, Chemotaxis of bacteria in glass capillary arrays, *Biophys. J.*, **58**(4), pp. 919–930, 1990.

35. A.L. Lin, B.A. Mann, G. Torres-Oviedo, B.Lincoln, J. Kas, H.L. Swinney, Localization and extinction of bacterial populations under inhomogeneous growth conditions, *Biophys. J.*, **87**(1), pp. 75–80, 2004.

36. H.G. Othmer, A. Stevens, Aggregation, blowup and collapse: the ABC's of taxis in reinforced random walks, *SIAM J. Appl. Math.*, **57**(4), pp. 1044–1081, 1997.

37. L.A. Pratt, R. Kolter, Genetic analysis of Escherichia coli biofilm formation: roles of flagella, motility, chemotaxis and type I pili, *Mol. Microbiol.*, **30**(2), pp. 285–293, 1998.